Role of Humic Acid Fraction with Higher Aromaticity in Enhancing the Activity of a Biomimetic Catalyst, Tetra(*p*-sulfonatophenyl)porphineiron(III)

Masami Fukushima,*,† Yasuaki Tanabe,‡ Kengo Morimoto,‡ and Kenji Tatsumi‡

Division of Solid Waste, Resources and Geoenviromental Engineering, Graduate School of Engineering, Hokkaido University, Sapporo 060-8628, Japan, and National Institute of Advanced Industrial Science and Technology (AIST), 16-1 Onogawa, Tsukuba-West, Tsukuba 305-8569, Japan

Received August 28, 2006; Revised Manuscript Received November 19, 2006

To elucidate the structural features of humic acids (HAs) that potentially contribute to enhancing the activity of a tetra(*p*-sulfonatophenyl)porphineiron(III) (Fe(III)-TPPS) catalyst, the effects of the chemical properties of molecular weight fractionated HAs on the catalytic activity of Fe(III)-TPPS were investigated. Three fractions were obtained as the following order of molecular size: F3 < F2 < F1. The deactivation of Fe(III)-TPPS, which can be attributed to the self-degradation of Fe(III)-TPPS, was retarded in the presence of HAs, and the pseudo-first-order rate constant in the presence of F3 was the smallest of the three fractions. In addition, the highest catalytic activity, determined as the percent degradation of an organic substrate, was observed in the presence of F3. The enhanced catalytic activity of Fe(III)-TPPS was due to the formation of supramolecular complexes with HAs, and the formation constant for F3 was the largest. Thus, the F3 fraction was the most effective fraction. Solid-state CPMS ^{13}C NMR spectra indicated that the aromaticity of F3 was the highest of all of the fractions. Thus, it can be concluded that aromatic moieties in HAs play an important role in the formation of supramolecular complexes with Fe(III)-TPPS, leading to an enhancement in catalytic activity.

Introduction

Humic acids (HAs) play important roles in facilitating remedial processes in soil and aquatic environments that are contaminated by organic pollutants. Because the photoexcitation of chromophores in HAs can produce active oxygen species (e.g., singlet oxygen, hydrogen peroxide, and hydroxyl radicals), the photolysis of pesticides, such as atrazine and 2,4,6-trimethylphenol, is facilitated in the presence of HAs.[1,2] In addition, redox moieties in HAs, such as quinone/hydroquinone redox couples, are involved in enhancing the reductive dehalogenation of trichloroethylene, hexachloroethane, carbon tetrachloride, and bromoform.[3−5]

HAs are naturally occurring supramolecular structures derived from associations of relatively small heterogeneous molecules.[6−8] Because of the chemical complexity, variable chemical composition, and polydispersity of HAs, it is difficult to identify the specific structural features that are responsible for facilitating remedial processes. Elucidating the effective structures in HAs is of crucial importance for their application to soil remediation. The separation and characterization of HAs are a key to developing a better understanding of their functions for remedial processes in the environment. Size-exclusion chromatography (SEC) is frequently used to characterize HAs due to its ease of application, sensitivity, reproducibility, and availability.[9−11] To understand the roles of HAs in remedial processes, the effects of the structural features of molecular weight fractionated HAs on the photolysis and ozonation of organic pollutants were examined.[2,12]

We recently found that the addition of HAs to a biomimetic catalytic system, in which a tetra(*p*-sulfonatophenyl)porphineiron(III) (Fe(III)-TPPS) catalyst was used, led to the facilitation of the oxidation of pentachlorophenol.[13−15] As an approach to elucidating such effects of HA, cyclodextrins were used as model polysaccharide moieties in HAs. These experiments indicated that the formation of supramolecular complexes between the hydrophobic cores of cyclodextrins and sulfonatophenyl groups in Fe(III)-TPPS prevented the self-degradation of Fe(III)-TPPS, and this resulted in an enhancement in catalytic activity.[16,17] The aim of the present study was to elucidate the structural features of HAs that are effective for forming supramolecular complexes with Fe(III)-TPPS and enhancing catalytic activity. Therefore, an HA sample was fractionated by SEC, and each fraction was then chemically characterized. In addition, the effects of the structural features of fractionated HAs on catalytic activity and their ability to complex with Fe(III)-TPPS were investigated.

Experimental Section

Materials. Fe(III)-TPPS was synthesized by a method reported by Kawasaki et al.[18] The formula weight and the results of elemental analyses for the Fe(III)-TPPS are summarized in the Supporting Information (Table 1S). $KHSO_5$ was obtained as a triple salt, $2KHSO_5 \cdot KHSO_4 \cdot K_2SO_4$ (Merck). Pentachlorophenol (PCP, 99.0% purity) was purchased from Aldrich, and a stock solution (0.01 M) was prepared in acetonitrile. Citric acid monohydrate, $NaH_2PO_4 \cdot 2H_2O$, and Na_2HPO_4 (Nacalai Tesque) were used for preparing buffer solutions. All aqueous solutions were prepared using ultrapure water, obtained from a Milli-Q system (Millipore).

HA Samples. An HA sample was extracted from a peat soil (Shinshinotsu, Japan) and purified by the method approved by the International Humic Substances Society.[19] A powdered sample of the HA (10 mg) was dissolved in aqueous 0.01 M NaOH (10 mL), and the pH was adjusted to 8.0 with 1 M H_3PO_4. A 10 mL aliquot of this

* Corresponding author. Telephone: +81-11-706-6304. Fax: +81-11-706-6304. E-mail: m-fukush@eng.hokudai.ac.jp.
† Hokkaido University.
‡ AIST.

10.1021/bm060829r CCC: $37.00
Published on Web 01/10/2007

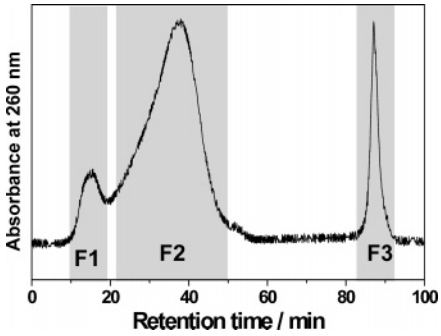

Figure 1. Gel permeation chromatogram of HA. Column size 30 mm ø × 300 mm, eluent 0.01 M phosphate buffer (pH 7) + 25% acetonitrile, sample volume 10 mL, sample concentration 1 g L^{-1}, flow rate 1.85 mL min^{-1}.

sample was injected into a preparative LC pumping system (YFLC-5404-FC-GRII type, Yamazen Co. Ltd.). The mobile phase consisted of a mixture of acetonitrile and aqueous 0.01 M phosphate buffer at pH 8 (25/75 = v/v), and the flow rate was set at 1.8−1.9 mL min^{-1}. A column (30 mm i.d. × 300 mm), packed with TOYOPEARL HW-55 gel (particle size 30−60 μm, exclusion limit 7×10^5 daltons, Tosoh Co. Ltd.), was used as the solid phase. The eluted HA was monitored by UV absorption at a wavelength of 260 nm. As shown in the chromatogram (Figure 1), three peaks were observed. Fractions corresponding to each peak (F1, F2, and F3) were collected using an FR-50N type fraction collector (Yamazen Co. Ltd.). The separation and collection of the fractions were repeated 102 times, and the collected fractions were stored frozen in polyethylene bottles. The acetonitrile in the collected fractions was removed by a rotary evaporator at 35 °C. The pH of the aqueous solution was then adjusted to 1 by adding 6 M HCl, and the resulting solution was then stirred for 24 h. The precipitate was separated by centrifugation (10 000 rpm, 15 min) and redissolved in 0.1 M NaOH. The pH of this solution was adjusted to pH 1 with 6 M HCl. After centrifugation, the precipitate was transferred to a dialysis tube (molecular weight cutoff of 500 Da, Spectra/Pore). To remove excess Cl^-, the dialysis was carried out against fresh ultrapure water, which was changed at 24 h intervals, for 2−3 weeks. The HA samples were obtained as a powder by lyophylization. In the present study, a total of 1020 mg of HA (102 times × 10 mg) was injected onto the column. Thus, 340 mg of each fraction would be expected to be recovered. However, as shown in Figure 1, some colored components in the HA were lost during the collection of the fractions. In addition, the adsorption of the HA to the gel particles and the complicated purification steps resulted in some loss of HA. Therefore, the final yields of the fractions were smaller than expected: F1, 100 mg; F2, 219 mg; F3, 48 mg.

Analyses of HAs. *Elemental Analyses.* The elemental compositions (C, H, N, S, and ash content) were determined at the Center for Instrumental Analysis at Hokkaido University (Sapporo, Japan). The percentage of oxygen was calculated by subtracting the sum of percentages of C, H, N, S, and ash from 100%.

Acidic Functional Groups. Total acidity and carboxylic group content were determined by the $Ba(OH)_2$ and $Ca(CH_3COO)_2$ methods, respectively.[20] The phenolic hydroxyl group content was calculated by subtracting the carboxylic group content from the total acidity.

Size Exclusion Chromatography. The molecular weights of the HAs were determined by SEC using an analytical column (A TSK-Gel α-M column, 7.8 mm i.d. × 300 mm, void volume 6.12 mL, Tosoh Co. Ltd.). Polystyrene sulfonic acid sodium salts (Fulka, molecular weight: 1400, 4300, 6800, 17 000, 32 000, 49 000, 77 000, 150 000, 350 000, and 990 000) were used as standard materials for the calibration of molecular weight. To estimate the apparent molecular weight (M) of all HA samples, a calibration curve was constructed on the basis of the observed linear relationship between the retention time corresponding to the highest peak and the actual log M for each standard material. The weight average molecular weight (M_W) was determined using the following equation:

$$M_W = \sum_{i=1}^{N} (h_i \cdot M_i) / \sum_{i=1}^{N} h_i$$

where h_i is the height of the sample signal and M_i is the molecular weight corresponding to the appropriate retention time.[21] A 20 μL aliquot of an aqueous solution of HA (250 mg L^{-1} in 0.1 M phosphate buffer at pH 7) was injected into a PU-980 type HPLC system (Japan Spectroscopic Co., Ltd.). The mobile phase consisted of a mixture of 0.1 M phosphate buffer (pH 7.0) and acetonitrile (75/25 = v/v), and the flow rate was set at 1.0 mL min^{-1}. The column temperature was maintained at 40 °C, and a UV-970 UV−vis detector (Japan Spectroscopic Co., Ltd.) was used for detection at a wavelength of 260 nm. All chromatograms were interpreted using the JASCO-BORWIN software (Japan Spectroscopic Co., Ltd.).

Spectroscopic Parameter. UV−vis absorption spectra of aqueous solutions of HAs (25 mg L^{-1} at pH 6 by 0.01 M phosphate buffer) were obtained on a Jasco V-550 type spectrophotometer (Japan Spectroscopic Co., Ltd.) using a 1 cm × 1 cm quartz cell. The absorptivities (E) at 465 and 665 nm were calculated as:

$$E\ (\mathrm{L\ cm^{-1}\ g^{-1}\ C}) = \frac{\text{absorbance}}{[\mathrm{HA\ (g\ L^{-1})}] \times \%\mathrm{C}/100}$$

^{13}C NMR Spectra. Solid-state CPMAS ^{13}C NMR spectra were acquired on a Chemagnetics CMX-300 spectrometer, equipped with a 5 mm CPMAS probe. An approximately 20 mg portion of HA powder was packed into a 5-mm zirconium rotor. The acquisition parameters were as follows: spectral frequency, 75.6 MHz for ^{13}C and 300.5 MHz for ^1H; contact time, 1 ms; pulse delay, 4 s; scan times, 20 000; line broadening, 50 Hz.

FTIR Spectra. FTIR spectra were recorded using a 460 Plus ST type FTIR spectrometer (Japan Spectroscopic Co., Ltd.) with KBr pellets.

UV−Vis Absorption Spectra of Fe(III)-TPPS. A 37.5 μL aliquot of aqueous 0.01 M $KHSO_5$ was added to 3 mL of the aqueous solution in a 1 × 1 cm quartz cell containing Fe(III)-TPPS (5 μM) and HA (50 mg L^{-1}) at pH 6 with stirring. The absorbance at 394 nm corresponding to the Soret band of Fe(III)-TPPS was then monitored for 1 min at 25 °C. To evaluate the conditional formation constants for the supramolecular complex between HAs and Fe(III)-TPPS, absorption spectra of aqueous solutions of Fe(III)-TPPS (5 μM) were recorded in the wavelength range of 300−700 nm at a variety of concentrations of HAs (0−70 mg L^{-1}) at 25 °C.

Catalytic Activity of Fe(III)-TPPS. To evaluate the catalytic activity of Fe(III)-TPPS, the degradation characteristics of PCP were evaluated. A 25 μL aliquot of 0.02 M phosphate/citrate buffer at pH 6, which contained 50 mg L^{-1} of HA, was placed in a 100-mL Erlenmeyer flask. A 125 μL aliquot of 0.01 M PCP in acetonitrile and a 625 μL aliquot of aqueous 200 μM Fe(III)-TPPS were added to the buffer solution. Subsequently, 313 μL of aqueous 0.01 M $KHSO_5$ was added, and the flask was then allowed to shake in a thermostatic shaking water bath at 25 ± 0.1 °C. After 5, 10, 20, 30, 45, and 60 min reaction periods, a 700 μL aliquot of the test solution was mixed with 350 μL of 2-propanol. To analyze for PCP in the solution, a 20 μL aliquot of the mixture was injected into a JASCO PU-980 type HPLC pumping system. The mobile phase consisted of a mixture of a 0.08% aqueous solution of H_3PO_4 and methanol (20/80 = v/v), and the flow rate was set at 1 mL min^{-1}. A 5C18-MS Cosmosil packed column (4.6 mm i.d. × 250 mm, Nacalai Tesque) was used as the solid phase, and the column temperature was maintained at 50 °C. PCP was detected by UV absorption at a wavelength of 220 nm. In addition, Cl^-, released during the oxidation of PCP, was determined by ion chromatography (DX-500 type, Dionex).

Results and Discussion

Characterization of Fractionated HAs. The weight average molecular weights (M_w) of the fractionated HAs are summarized

Table 1. Results of Elemental Analysis for Unfractionated (UF) and Fractionated HAs

HAs	%C	%H	%N	%O	%S	%ash	H/C	O/C
UF	54.52	5.35	2.17	35.08	0.66	2.22	1.17	0.48
F1	48.55	5.76	2.27	31.13	0.51	11.78	1.41	0.48
F2	52.96	4.64	2.38	35.09	1.00	3.93	1.04	0.50
F3	56.82	4.88	1.47	33.89	0.62	2.32	1.02	0.45

Table 2. Weight Average Molecular Weight (M_W), Spectroscopic Parameter, and Acidic Functional Group Content for HAs

			acidic functional groups (mequiv g^{-1} C)		
HAs	log M_W	log E_{465}/E_{665}	total acidity	carboxylic	phenolic hydroxyl
UF	3.72	0.82	10.45	3.15	7.34
F1	4.58	0.74	9.49	3.97	5.23
F2	3.75	0.91	12.50	5.39	7.11
F3	3.68	0.94	9.49	3.35	6.13

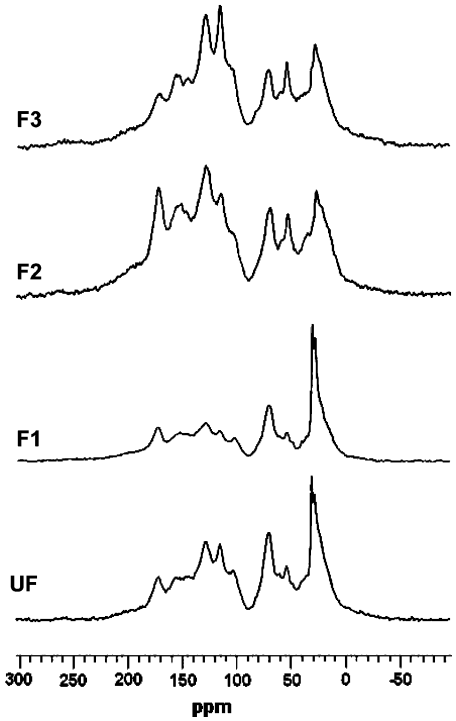

Figure 2. Solid-state CPMS ^{13}C NMR spectra of each fraction.

in Table 2. As would be expected from the chromatogram in Figure 1, the order of log M_w for each fraction was as follows: F3 < F2 < F1. The spectroscopic parameters of the HAs are also summarized in Table 2. It is known that log E_{465}/E_{665} decreases with increasing molecular weight of HA.[22] The order of the log E_{465}/E_{665} found in the present study was in general agreement with this conclusion. The H/C atomic ratio is known to be one of the indices of the degree of unsaturation of HAs.[23] As shown in Table 1, the H/C ratio for F1 was the largest of all of the HAs, suggesting that F1 contains larger amounts of saturated carbon (i.e., aliphatic carbons) as compared to the other HAs. Figure 2 shows the solid-state CPMS ^{13}C NMR spectra of HAs. In the spectrum of F1 and unfractionated HA (UF), sharp peaks corresponding to methyl carbons were observed in the range of 0−40 ppm. In particular, the peaks corresponding to aromatic carbons (105−160 ppm) for F1 were significantly smaller than those for the other HAs. To determine the carbon species more precisely, the spectral peaks were identified and integrated using the assignments reported by Wershaw et al.[24] The peak assignments and the percentages of carbon species in each sample are summarized in Table 3. The sum of the percent aliphatic carbons (0−90 ppm) for F1 (52.09%) was the largest of the three fractions (F2 37.81%; F3 39.81%). In addition, the sum of the percent aromatic carbons (105−160 ppm) for F2 (37.08%) and F3 (39.70%) was much larger than that for F1 (27.55%). These results show that F1 contains large amounts of aliphatic moieties, while F2 and F3 have more aromatic characteristics than F1. Figure 3 shows FTIR spectra of the HAs. The peaks at 2870 and 2930 cm^{-1} corresponding to the C−H stretching of methyl or methylene groups (D in Figure 3) and the peak at 1060 cm^{-1} corresponding to the C−O−C symmetrical stretching of ethers or the C−O stretching of alcohols (O in Figure 3) in F1 were the strongest of all of the HAs. These results support the conclusion that the F1 fraction has more aliphatic characteristics than F2 and F3.

The O/C atomic ratios for each HA are summarized in Table 1. The O/C ratio is a measure of the content of oxygen-containing functional groups, such as carboxylic acids, phenolic hydroxyl groups, alcoholic hydroxyl groups, and ethers.[25] As shown in Table 1, the O/C ratios for each HA fraction were not substantially different. However, the percent carbonyl carbon (160−180 ppm) for F2 was significantly larger than those for the other HAs (Table 3). As shown in Table 2, the total acidities for F2 and UF were larger than those for F1 and F3. In particular, the carboxylic group content of F2 was the largest of all of the HAs. These results indicate that F2 contains larger amounts of carboxylic acid groups as compared to the other HAs.

Kinetics of Self-Degradation of Fe(III)-TPPS. The deactivation of Fe(III)-TPPS may be due to aggregation and/or self-degradation in the presence of peroxides, such as H_2O_2 and $KHSO_5$.[26] It has been reported that the aggregation of Fe(III)-TPPS can yield m-oxo species, O-(Fe(III)-TPPS)$_2$, which are produced in higher concentrations of Fe(III)-TPPS and at a higher pH.[18,27] In our experimental conditions (5 mM Fe(III)-TPPS, pH 6), the wavelength corresponding to the absorption maximum for the Soret band of Fe(III)-TPPS (394 nm) was similar to that at pH 2, where aggregation could not occur. However, when the pH was increased to 7, the wavelength of the Soret band of Fe(III)-TPPS shifted from 394 to 406 nm, indicating the formation of O-(Fe(III)-TPPS)$_2$ species.[18] These results support the conclusion that aggregation does not cause any loss in catalytic activity under our experimental conditions. Therefore, this study focused on the self-degradation of Fe(III)-TPPS.

The self-degradation of Fe(III)-TPPS in the presence of $KHSO_5$ can be monitored by measuring the decolorization of the catalyst.[28] Figure 4 shows the kinetic curves for the self-degradation of Fe(III)-TPPS. The inset in Figure 4 shows the pseudo-first-order kinetics in the initial parts of the kinetic curves for the self-degradation of Fe(III)-TPPS. It has been reported that, after a 1 day degradation period, approximately 50% of the Fe(III)-TPPS is mineralized to CO_2, and approximately 10−20% of the carbon in Fe(III)-TPPS is converted to formic and oxalic acids.[16] This supports the conclusion that the decolori-

Table 3. Peak Assignments of Solid-State CPMS ^{13}C NMR Spectra of HAs and Rates of Carbon Species

		rate of carbon species (%)			
peaks (ppm)	assignments	UF	F1	F2	F3
	Aliphatic Carbon				
0−50	aliphatic carbon atoms	29.49	33.22	21.91	22.70
50−55	methyl esters	2.70	2.37	2.82	2.96
55−60	methyl ethers	2.20	2.01	1.86	2.28
60−90	aliphatic ethers and alcohols	14.76	14.49	11.22	11.87
	Anomeric Carbon				
90−105	anomeric carbon atoms	5.77	4.56	4.78	6.29
	Aromatic Carbon				
105−135	aromatic carbon atoms attached to proton or other carbon atoms	21.01	15.78	21.92	25.93
135−160	aromatic carbon atoms attached to oxygen atoms	11.75	11.77	15.16	13.77
	Carbonyl Carbon				
160−180	carbonyl carbons (acids)	7.44	8.91	11.95	7.85
180−220	carbonyl carbons (quinones)	4.88	6.88	8.38	6.35

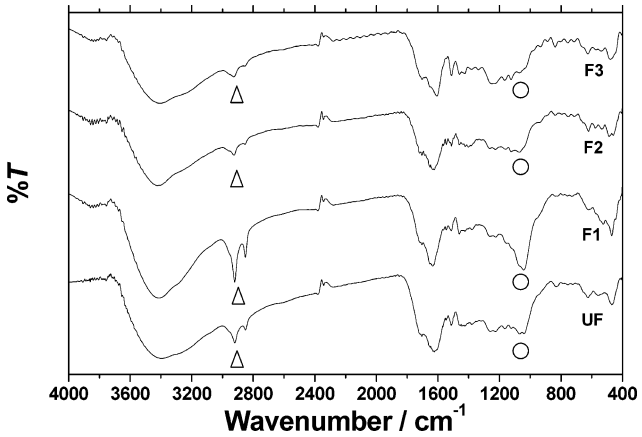

Figure 3. FTIR spectra of HAs with KBr disk.

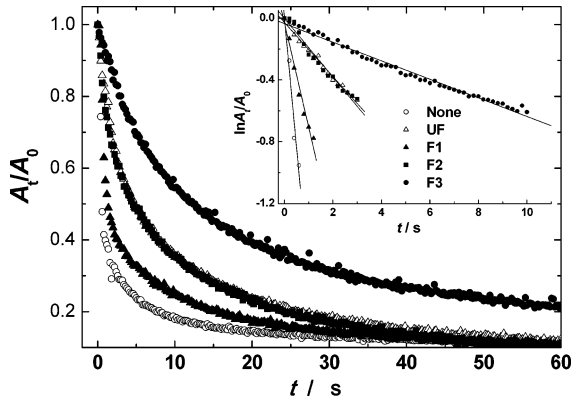

Figure 4. Kinetic curves for Fe(III)-TPPS self-degradation in the absence and presence of HA. The inset indicates the pseudo-first-order interpretation of initial rate of self-degradation. [Fe(III)-TPPS] 5 μM, [$KHSO_5$] 125 μM, [HA] 50 mg L^{-1} ([DOC] (mM): UF 2.3, F1 2.0, F2 2.3, F3 2.4), pH 6, 25 °C.

zation of Fe(III)-TPPS is due to the oxidative degradation of Fe(III)-TPPS in the presence of $KHSO_5$. However, the identification of the byproducts in the initial stage of the self-degradation was difficult, because the reaction rate was too high to permit the byproducts to be analyzed in situ.

To compare the samples from different origin, concentrations of HAs (g L^{-1}) are generally normalized to the concentrations of dissolved organic carbon (DOC).[29,30] The detailed process for the normalization is described in eq 6 in the Supporting Information. The calculated concentrations of DOC (mM) for each sample (UF 2.3, F1 2.0, F2 2.2, F3 2.4) suggest that pseudo-first-order rate constants (k) at [HA] = 50 mg L^{-1} in Table 4, which are calculated from the inset in Figure 4, are comparable with each other. Table 4 shows pseudo-first-order rate constants (k), calculated from the inset in Figure 4. The k values in the absence of HAs were significantly larger than those in the presence of HAs, suggesting that the addition of the HAs retarded the self-degradation of Fe(III)-TPPS. In the presence of HAs, the order for the k values was as follows: F3 < UF ≤ F2 < F1. In particular, the k value for F3 was 1 order of magnitude smaller than that of F1. These results suggest that F3 is the most effective fraction in retarding the self-degradation of Fe(III)-TPPS, while F1 is less effective than the other HAs.

Table 4. Initial Pseudo-First-Order Rate Constants for the Self-Degradation of Fe(III)-TPPS (k) and Conditional Formation Constants (K_f) for the Supramolecular Complexes of Fe(III)-TPPS with HAs

HAs	k (s^{-1})	log K_f
none	1.50 ± 0.30	
UF	0.16 ± 0.02	1.92 ± 0.02
F1	0.63 ± 0.06	1.63 ± 0.01
F2	0.20 ± 0.02	1.87 ± 0.01
F3	0.06 ± 0.01	2.14 ± 0.01

Oxidation of Organic Substrate. Piccolo et al.[31,32] reported that the phenolic constituents in HAs underwent oxidative coupling by an iron(III)-porphyrin catalyst in the presence of peroxides. This suggests that the retardation of the self-degradation of Fe(III)-TPPS occurs via competition with the oxidation of HAs. If the retardation in self-degradation was due to competition with the oxidation of HAs, the oxidation efficiencies for any of the organic substrates might decrease in the presence of HAs. This can be accomplished by comparing the degradation characteristics of organic substrates in the Fe(III)-TPPS/$KHSO_5$ catalytic system in the absence and presence of HAs. In the present study, PCP was used as an example of an organic substrate, because its oxidation products in the Fe(III)-TPPS/$KHSO_5$ catalytic system have been previously identified.[13,15,16]

Figure 5a and b shows the kinetics of PCP disappearance and Cl^- release in the absence and presence of HAs, respectively. The PCP rapidly disappeared within the first 5 min followed by a gradual decrease. Based on our current knowledge

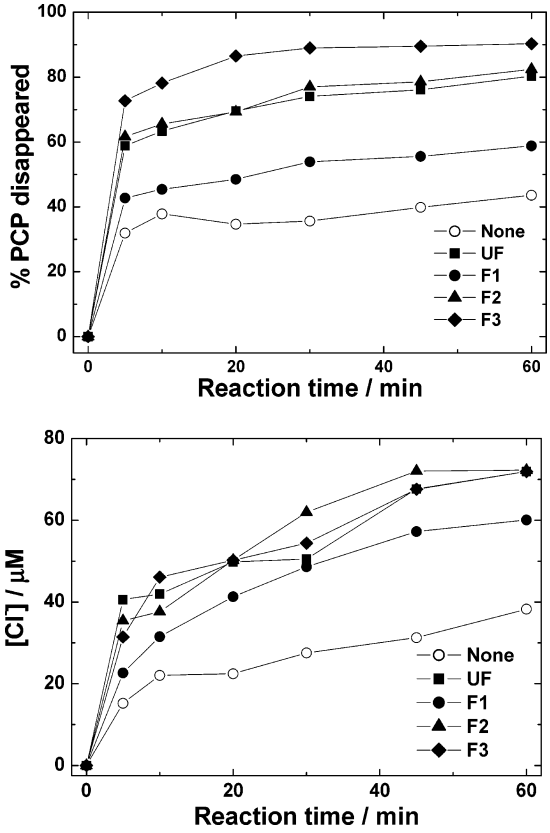

Figure 5. Kinetics of PCP disappearance (a) and dechlorination (b) in the absence and presence of HAs. [Fe(III)-TPPS] 5 μM, [$KHSO_5$] 125 μM, [PCP]$_0$ 50 μM, [HA] 50 mg L^{-1} ([DOC] (mM): UF 2.3, F1 2.0, F2 2.3, F3 2.4), pH 6, 25 °C.

of the oxidation of 2,4,6-trichlorophenol via the Fe(III)-TPPS/$KHSO_5$ catalytic system,[33] the formation of 2,4-dichloroquinone via a chlorophenoxy radical constitutes the initial rapid step and occurs within the first 5 min. Thus, the rapid parts in the kinetic curves, shown in Figure 5a, can be attributed to the formation of chloroquinone derivatives via the pentachlorophenoxy radical (PCP). In addition, it is known that PCP can be oxidized to dimers, such as hydroxyl-nonachlorodiphenyl ethers and octachlorodibenzo-*p*-dioxin.[13,15,16] As shown in Figure 5b, Cl^- was simultaneously released from PCP at a rapid rate during the first 5 min of the reaction, followed by a more gradual increase. This tendency in Figure 5b is consistent with the results shown in Figure 5a. For all data points, the molar ratios of [Cl^-] released to [PCP] disappearance were in the range of 1.0−2.3. Therefore, the expected byproducts, in which 1−2 chlorine atoms had been released from PCP, are consistent with the previously reported analytical results.[13,15,16] These results support the conclusion that the disappearance of PCP, observed in Figure 5a, can be attributed to dechlorination via catalytic oxidation in the Fe(III)-TPPS/$KHSO_5$ system.

As shown in Figure 5a, the percentage of PCP disappearance at all reaction periods in the absence of HAs was significantly smaller than those in the presence of HAs. These results clearly prove that the retardation in the self-degradation of Fe(III)-TPPS, observed in Figure 4, cannot be attributed to competition by the oxidation of HAs. In the presence of HAs, the percent PCP disappearance for F3 was the largest of all of the HAs, showing that F3 is the most effective in enhancing the catalytic activity of Fe(III)-TPPS. Such a trend is consistent with the conclusion that F3 is the most effective for retarding the self-degradation of Fe(III)-TPPS.

Formation of Supramolecular Complexes. The formation of supramolecular complexes between Fe(III)-TPPS and HAs may play an important role in the retardation of self-degradation of the catalyst in the presence of $KHSO_5$. Therefore, complexation between Fe(III)-TPPS and HAs was investigated by observing the UV−vis absorption spectra of the Soret band for Fe(III)-TPPS in the absence and presence of HAs. The conditional formation constant for the supramolecular complex (K_f) was evaluated, based on the decrease in the absorbance of the Soret band of Fe(III)-TPPS with increasing concentrations of HAs. The detailed processes for evaluating K_f values are described in the Supporting Information. As listed in Table 4, the order of log K_f values was as follows: F1 < F2 ≤ UF < F3. This shows that F3, which is effective in retarding the self-degradation of Fe(III)-TPPS and in enhancing PCP degradation, has the strongest binding ability to Fe(III)-TPPS. In addition, the log K_f values were negatively correlated with the logarithms of the k values ($r^2 = 0.999_8$). These results support the conclusion that the formation of supramolecular complexes between Fe(III)-TPPS and HAs contributes to the retardation in the self-degradation of Fe(III)-TPPS.

Burley and Petsko[34] proposed a specific aromatic−aromatic interaction between side aromatic residues in some peptides relating to quadrupole−quadrupole interactions. In addition, Zhu et al.[35] demonstrated that $\pi-\pi$ electron donor−acceptor interactions play an important role in aromatic−aromatic interactions between aromatic compounds and aromatic moieties in soil organic matter. In the present study, both the log K_f value and the aromaticity of F3 were the largest of all of the samples. This suggests that the formation of supramolecular complexes is mainly due to aromatic−aromatic interactions between sulfonatophenyl groups in Fe(III)-TPPS and aromatic moieties in HAs. However, F1, which included larger amounts of aliphatic moieties, had the smallest log K_f value. Therefore, aliphatic components in HAs are less responsible for interactions with Fe(III)-TPPS than are aromatic moieties.

As shown in Table 3, the aromaticity for F2 (37.1%) was not substantially different from that for F3 (39.7%). Nevertheless, the catalytic activity and binding ability to Fe(III)-TPPS for F3 were clearly higher than those for F2. A significant difference in structural features between F2 and F3 was that the level of carboxylic groups in F2 was much higher than that in F3. We previously investigated the influence of HA type, in terms of enhancing PCP degradation in the Fe(III)-TPPS/$KHSO_5$ system.[14] In this study, HAs with higher contents of carboxylic groups were not effective in enhancing PCP oxidation. It is known that the large negative electrostatic fields of HAs are mainly due to the presence of carboxylic acid groups. Under our experimental conditions (pH 6), the majority of the carboxylic acids in HAs would be dissociated into carboxylate anions.[36,37] Thus, both Fe(III)-TPPS and HAs have negative charges and would be expected to bind weakly to each other because of electrostatic repulsion. Although the levels of aromaticity for F2 and F3 were similar, the binding ability to Fe(III)-TPPS to F3 was much larger than that for F2. This can be attributed to the fact that the carboxylic group content (i.e., negative charge density) of F2 was larger than that of F3. Therefore, the level of carboxylic groups in HAs, as well as the degree of aromaticity, was an important factor in the formation of supramolecular complexes with Fe(III)-TPPS.

Our study led to the conclusion that characters of the fraction for enhancing the catalytic activity of Fe(III)-TPPS were of a higher aromaticity and a smaller negative charge density. The formation of supramolecular complexes can be attributed to

aromatic−aromatic interactions between sulfonatophenyl groups in Fe(III)-TPPS and aromatic moieties in HAs. Piccolo et al. reported that the conformational rigidity of HA aggregates increased as a result of oxidation with an iron(III)-porphyrin catalyst via the oxidative coupling of small phenolic moieties in HAs.[31] They also suggested that aromatic regions in iron-(III)-porphyrin catalyst are covalently incorporated into HA via oxidative coupling. Although the formation constants of supramolecular complexes were measured in the absence of $KHSO_5$ in the present study, covalent binding, as suggested by Piccolo et al.,[31] would be expected in the presence of $KHSO_5$. However, Fe(III)-TPPS was ultimately decolorized by $KHSO_5$ even in the presence of HAs. Thus, the enhanced catalytic activity of Fe(III)-TPPS reported here is mainly due to the retardation in the self-degradation of Fe(III)-TPPS as a result of the formation of supramolecular complexes via aromatic−aromatic interactions. The findings herein provide useful information for the application of HAs to soil remediation using biomimetic catalysts, such as iron(III)-porphyrins.[38]

Acknowledgment. This work was supported by Grants-in-Aid for Scientific Research from the Japan Society for the Promotion of Science (18201013).

Supporting Information Available. Evaluation of the conditional formation constant (K_f) of the supramolecular complexes between Fe(III)-TPPS and HAs, and formula weight and results of elemental analyses of the Fe(III)-TPPS synthesized (Table 1S). This material is available free of charge via the Internet at http://pubs.acs.org.

References and Notes

(1) Prosen, H.; Zupančič-Kralj, L. *Environ. Pollut.* **2005**, *113*, 517−529.
(2) Richard, C.; Trubetskaya, O.; Trubetskoj, O.; Reznikova, O.; Afanas'Eva, G.; Aguer, J.-P.; Guyot, G. *Environ. Sci. Technol.* **2004**, *38*, 2052−2057.
(3) O'Loughlin, E. J.; Burris, D. R.; Delcomyn, C. A. *Environ. Sci. Technol.* **1999**, *33*, 1145−1147.
(4) Ma, H.; O'Loughlin, E. J.; Burris, D. R. *Environ. Sci. Technol.* **2001**, *35*, 717−724.
(5) Curtis, G. P.; Reinhard, M. *Environ. Sci. Technol.* **1994**, *28*, 2393−2401.
(6) Conte, P.; Piccolo, A. *Environ. Sci. Technol.* **1999**, *33*, 1682−1690.
(7) Piccolo, A. *Adv. Agron.* **2002**, *75*, 57−134.
(8) Smeulders, D. E.; Wilson, M. A.; Kamali Kannangara, G. S. *Org. Geochem.* **2001**, *32*, 1357−1371.
(9) Guggenberger, G.; Kögel-Knabner, I.; Haumaier, L.; Zech, W. *Sci. Total Environ.* **1989**, *81/82*, 447−457.
(10) Conte, P.; Piccolo, A. *Chemosphere* **1999**, *38*, 517−528.
(11) Peuravuori, J.; Pihlaja, K. *Anal. Chim. Acta* **1997**, *337*, 133−149.
(12) These, A.; Reemtsma, T. *Environ. Sci. Technol.* **2005**, *39*, 8382−8387.
(13) Fukushima, M.; Ichikawa, H.; Kawasaki, M.; Sawada, A.; Morimoto, K.; Tatsumi, K. *Environ. Sci. Technol.* **2003**, *37*, 386−394.
(14) Fukushima, M.; Sawada, A.; Kawasaki, M.; Ichikawa, H.; Morimoto, K.; Tatsumi, K.; Aoyama, M. *Environ. Sci. Technol.* **2003**, *37*, 1031−1036.
(15) Rismayani, S.; Fukushima, M.; Sawada, A.; Ichikawa, H.; Tatsumi, K. *J. Mol. Catal. A* **2004**, *217*, 13−19.
(16) Fukushima, M.; Tatsumi, K. *Environ. Sci. Technol.* **2005**, *39*, 9337−9342.
(17) Fukushima, M.; Tatsumi, K. *J. Mol. Catal. A* **2006**, *245*, 178−184.
(18) Kawasaki, M.; Kuriss, A.; Fukushima, M.; Sawada, A.; Tatsumi, K. *J. Porphyrins Phthalocyanines* **2003**, *7*, 645−650.
(19) Swift, R. S. In *Methods of Soil Analysis Part 3. Chemical Methods*; Sparks, D. L., Page, A. L., Helmke, P. A., Loeppert, R. H., Soltanpour, P. N., Tabatabai, M. A., Johnson, C. T., Summer, M. E., Eds.; Soil Science Society of America: Madison, 1996; pp 1018−1020.
(20) Schnitzer, M.; Khan, S. U. *Humic Substances in the Environment*; Dekker: New York, 1972; pp 37−43.
(21) Hur, J.; Williams, M. A.; Schlautman, M. A. *Chemosphere* **2006**, *63*, 387−402.
(22) Chen, Y.; Senesi, N.; Schnitzer, M. *Soil Sci. Soc. Am. J.* **1977**, *41*, 352−358.
(23) Kuwatsuka, S.; Tsutsuki, K.; Kumada, K. *Soil Sci. Plant Nutr.* **1978**, *24*, 337−347.
(24) Wershaw, R. L.; Kennedy, K. R.; Henrich, J. E. In *Humic Substances. Structures, Properties and Uses*; Davies, G., Ghabbour, E. A., Eds.; The Royal Society of Chemistry: Cambridge, 1998; pp 29−46.
(25) Tsutsuki, K.; Kuwatsuka, S. *Soil Sci. Plant Nutr.* **1978**, *24*, 547−560.
(26) Lindsay Smith, J. R. In *Metalloporphyrins in Catalytic Oxidations*; Sheldon, R. A., Ed.; Dekker: New York, 1994; pp 325−327.
(27) Fleischer, E. B.; Palmer, J. M.; Srivastava, T. S.; Chatterjee, A. *J. Am. Chem. Soc.* **1971**, *93*, 3162−3167.
(28) Nappa, M. J.; Tolman, C. A. *Inorg. Chem.* **1985**, *24*, 4711−4719.
(29) Chiou, C. T.; Malcolm, R. L.; Brinton, T. I.; Kile, D. E. *Environ. Sci. Technol.* **1986**, *20*, 502−508.
(30) Nakayasu, K.; Fukushima, M.; Sasaki, K.; Tanaka, S.; Nakamura, H. *Environ. Toxicol. Chem.* **1999**, *18*, 1085−1090.
(31) Piccolo, A.; Conte, P.; Tagliatesta, P. *Biomacromolecules* **2005**, *6*, 351−358.
(32) Smejkalová, D.; Piccolo, A. *Environ. Sci. Technol.* **2006**, *40*, 1644−1649.
(33) Shukla, R. S.; Robert, A.; Meunier, B. *J. Mol. Catal. A* **1996**, *113*, 45−49.
(34) Burley, S. K.; Petsko, G. A. *Science* **1985**, *229*, 23−28.
(35) Zhu, D.; Hyun, S.; Pignatello, J. J.; Lee, L. S. *Environ. Sci. Technol.* **2004**, *38*, 4361−4368.
(36) Fukushima, M.; Tanaka, S.; Hasebe, K.; Taga, M.; Nakamura, H. *Anal. Chim. Acta* **1995**, *302*, 365−373.
(37) Terashima, M.; Fukushima, M.; Tanaka, S. *Colloids Surf., A* **2004**, *247*, 77−83.
(38) Chen, S.-T.; Stevens, D. K.; Kang, G. *Water Res.* **1999**, *33*, 3657−3665.

BM060829R